Iraqi Journal of Physics, 2018 *Vol.16, No.38, PP. 124-131*

DOI: 10.20723/ijp.16.38.124-131

Synthesis and characterization of nanocrystalline copper sulfide powders

Ulla M. Sleman and Iqbal S. Naji

Department of Physics, College of Science, University of Baghdad

E-mail: moonbb_moonaaaa@yahoo.com

Abstract

Nanocrystalline copper sulphide ($Cu_{2-x}S$) powders were synthesized by chemical precipitation from their aqueous solutions composed of different molar ratio of copper sulfate dehydrate ($CuSO_4.5H_2O$) and thiorea $(NH_2)_2CS$ as source of Cu^{+2}, S^{-2} ions respectively, and sodium ethylene diamine tetra acetic acid dehydrate (EDTA) as a complex agent. The compositions, morphological and structural properties of the nanopowders were characterized by energy dispersive spectroscopy (EDS), scanning electron microscope (SEM), and X-ray diffraction (XRD), respectively. The compositional results showed that the copper content was high and the Sulfur content was low for both CuS and Cu_2S nanopowders. SEM images shows that all products consist of aggregate of fine nanospheres with uniform distribution and the size of the particles formed are in nanometer range. XRD results revealed that the obtained powders contains a mixture of copper sulfide phases specially the intermediate phases and the rough estimate of the average crystallite size using the Scherrer formula gives a range of values (4.1-36.9) nm.

Key words

Copper sulfide, composition and morphological properties, structural properties.

Article info.

Received: Apr. 2018
Accepted: May. 2018
Published: Sep. 2018

تحضير و خصائص مساحيق كبريتيد النحاس النانويه

علا مظفر سليمان و إقبال سهام ناجي

قسم الفيزياء، كلية العلوم، جامعة بغداد

الخلاصة

تم تحضير مساحيق كبريتيد النحاس النانويه بطريقة الراسب الكيميائي من المحاليل المائية والتي تحتوي على نسب مولارية مختلفة من كبريتات النحاس والثايوريا كمصدر لايونات النحاس والكبريت على التوالي، واستخدم EDTA كعامل معقد للتفاعل. تم دراسة المكونات والخصائص السطحية والتركيبية للمساحيق النانويه باستخدام مطياف تفريق الطاقة، المجهر الالكتروني الماسح و حيود الأشعة السينية على التوالي. أظهرت نتائج المكونات بان هناك محتوى عالي من النحاس ومحتوى منخفض من الكبريت ولكلا المسحوقين CuS و Cu_2S. اما صور المجهر الالكتروني الماسح فقد أظهرت بان كل المساحيق الناتجة تحتوي على تجمعات من الكرات النانويه الدقيقة مع توزيع متجانس وان حجم الجسيمات المتكونة في مدى الإبعاد النانويه. اظهرت نتائج الأشعة السينية بان المساحيق المستحصلة تتكون من خليط من أطوار كبريتيد النحاس وخاصة الاطوار الوسطية وان تقدير معدل حجم البلورات باستخدام صيغة شيرر تعطي معدل من القيم تتراوح بين 4.10 الى 36.90 نانومتر.

Introduction

The development of nanostructured materials in the form of thin films has appropriate place in the research of solid state technology, it has high surface area to volume ratio therefore it have different structural, optical, electrical, magnetic and dielectric properties than bulk [1]. The nanomaterials especially metal

chalcogenides, like selenides, sulfides, and telluride are being studied widely due to their quantum confinement effects that associated to their small crystalline size [2, 3], which give them a large potential applications in the light emitting diodes, solar cells, fuel cell, drug delivery, catalysts for industrial transformation, gas and photo-sensing mechanism [2, 4].

The transition sulfides metal are very promising semiconducting materials that have been used in many applications due to their excellent properties that includes a unique structure morphology, direct band gap, and high absorption coefficient of more than 10^5 cm^{-1} [5].

$Cu_{2-x}S$ nanocrystals act as p-type semiconductor material mainly due to that of copper vacancies occurring within the lattice, which is the reason for their use in optoelectronic devices [6]. It is also used in photothermal conversion applications, solar control coatings, photovoltaic applications, electronic devices, optical filters as well as in low temperature gas sensor applications [7, 8].

Copper sulfide ($Cu_{2-x}S$) has five stable phases that naturally occurs depends on the varying of Cu/S ratio, Covellite (CuS), anillite ($Cu_{1.75}S$), degenite ($Cu_{1.8}S$), djurelite ($Cu_{1.95}S$), and chalcocite (Cu_2S) [9], Other phases that exist include yarowite ($Cu_{1.12}S$) and spionkopite ($Cu_{1.14}S$) [7].

The synthesis of Copper sulfide nanoparticles by a simple method is still a challenge [10]. Many methods have been developed to synthesize copper sulphide nanoparticles such as microwave [11], solvothermal [12], electrosynthesis [13], organometallic precursor route [14], hydrothermal [15], and chemical precipitation [16].

The present paper deals with the synthesis $Cu_{2-x}S$ nanocrystalline powders with different molar ratio of Cu/S, and study the compositional, structural, and morphological properties of these powders.

Experimental

$Cu_{2-x}S$ nanocrystalline powders were obtained by chemical precipitation from their aqueous solutions composed of different molar ratios of Cu, using copper sulfate pent hydrate ($CuSO_4.5H_2O$), thiorea ($(NH_2)_2CS$) as source of Cu^{+2}, S^{-2} ions respectively, with disodium ethylenediamine tetraacetate ($Na_2EDTA.2H_2O$). To maintain basic medium, ammonium hydroxide (NH_4OH) was used to adjust PH of the solution.

The procedure for prepare CuS film involve, taking 15 ml of copper salt solution as Cu^{+2} ion source in 100ml beaker, 15 ml of complex agent is mixed drop wise , the solution is stirred constantly for few min for getting homogenous mixture. Then add NH_4OH drop wise until the color of the solution changes from light blue to dark blue (pH=10). After this 15ml of thiorea add as S^{-2} ion source, stir the solution for 15 min, then the solution color become olive. The reaction mixture keep in water bath at 60 ^oC. After 90 min the reaction was completed and the particles settled down at the bottom of the beaker. During the precipitate formation a change in color from purple-silver to black was observed. The as synthesized product was filtered and rinsed several times with distilled water, then it was dried in oven at 100 ^oC for 1hr to obtain powder.

Five reaction baths were used trying to obtain different copper sulfide powders with different phases (CuS, $Cu_{1.75}S$, $Cu_{1.8}S$, $Cu_{1.95}S$ and Cu_2S) by changing Cu/S molar ratio in the solution.

The compositional, structural, and morphological properties of the prepared powder were studied. Compositions of elements were

recorded by EDS, type Bruker company- Germany, X-Flash 6l10-model (Physics Department, College of Science, Al-Nahrain University), and x-ray diffraction was determined by (Miniflex II Rigaku company, Japan) diffractometer equipped with a Cu-Kα radiation. The morphological features for the prepared powders were studied by scanning electron microscopy (SEM), model (TOSHIBA 4160), with high resolution mode, accelerating voltage (200 eV and 30 keV), and SEM magnification from (3-1000000).

Results and discussion

The elemental composition of $Cu_{2-x}S$ powders for different values of x (1, 0.25, 0) were investigated using EDX and the charts are shown in Fig. 1. Peaks of Cu and S exhibit the presence of these elements in these powders.

There are small peaks of Oxygen, Nitrogen and Carbon originated from the precursor material which are used in the chemical reaction or from the contaminated with the elements exist in the environment.

The elemental analysis was carried out only for Cu and S and the mass percentage of Cu:S in these powders were calculated and listed in Table 1.

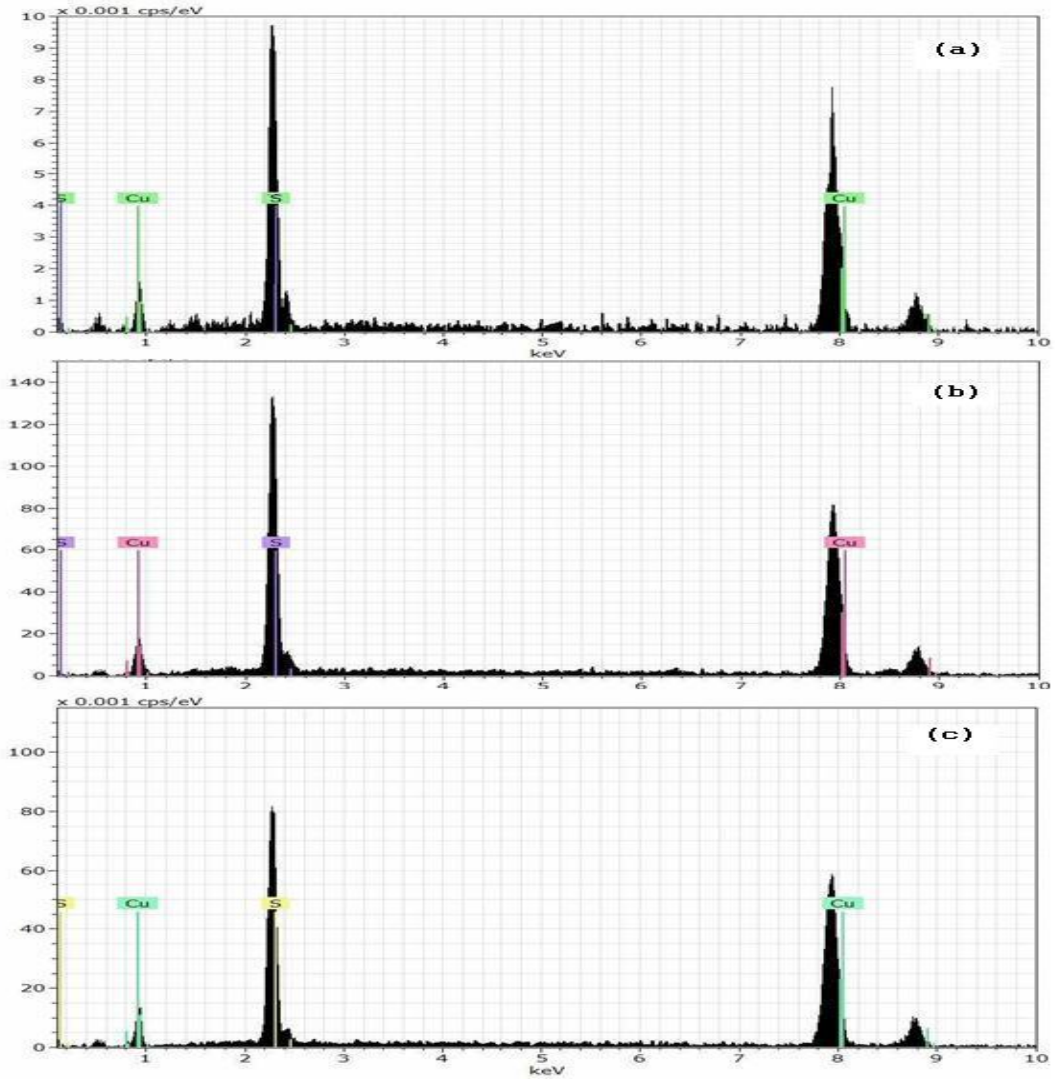

Fig. 1: EDS chart of $Cu_{2-x}S$ powders at different ratios of Cu: a-x=1, b-x=0.25, c-x=0.

Table 1: The elemental analysis for $Cu_{2-x}S$ powders prepared by chemical bath deposition method at different ratios of Cu.

Sample	Element	A. mass	No. of atoms	Mass percent (The.)	Mass percent (Exp.)
CuS	Cu	63.546	1	66.46	70.25
	S	32.065	1	33.53	29.75
$Cu_{1.75}S$	Cu	63.546	1.75	77.65	71.82
	S	32.065	1	22.38	23.28
Cu_2S	Cu	63.546	2	79.85	83.0
	S	32.065	1	20.14	11.78

It is clear that the composition ratio of the elements deviation from the calculated ratio, where the copper ratio was high in the CuS and Cu_2S powders and the sulfur was low content. This is may be occurs because of the interaction between copper and complex agent, which may effect the operation of released ions that can be high. In different way sulfur was bound in solution after the reaction, therefore the ratio of sulfur was low.

Scanning electron microscopy is a convenient method to study the surface morphology of powder and thin films. It gives as important information regarding growth, shape and size of the particles. Surface morphology of material plays an important role in solar energy conversion efficiency of the device.

Fig. 2 shows the surface morphology of the $Cu_{2-x}S$ powders of different molar ratio (x=1, 0.25, 0) with different magnification. It was observed from these images that all products consist of aggregate of fine nanospheres with uniform distribution, the size of the particles formed are in nanometer range.

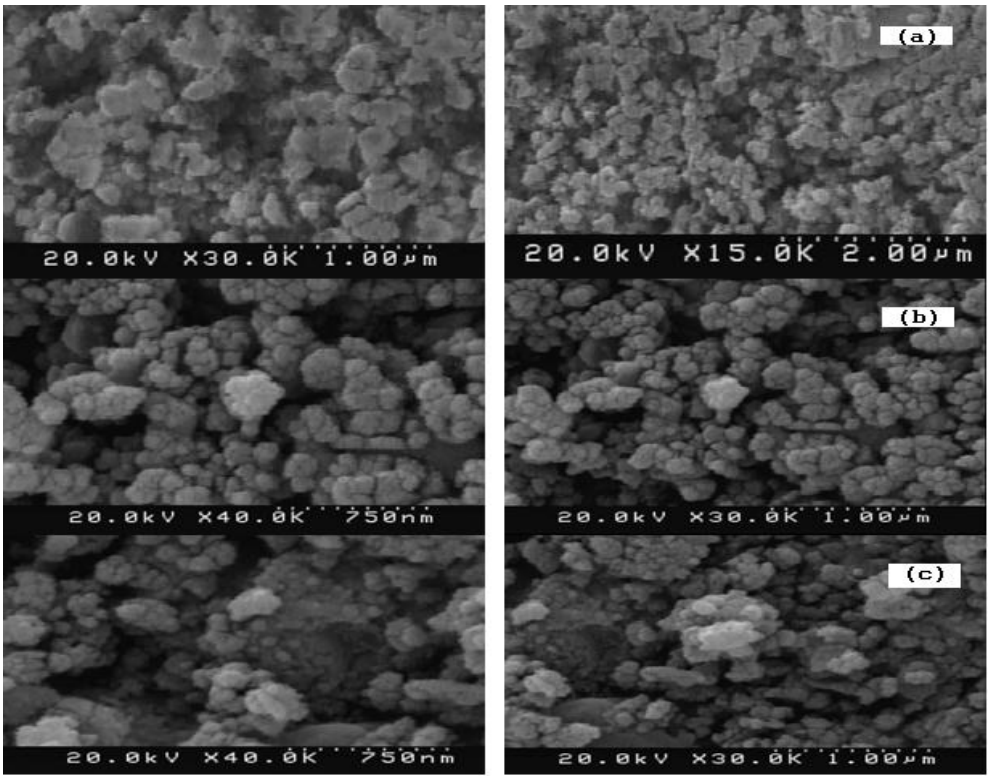

Fig. 2: SEM photograph of $Cu_{2-x}S$ powders at different molar ratio of Cu: (a) x=1, (b)x=0.25, (c)x=0.

The structure of $Cu_{2-x}S$ powders of different molar ratio of Cu were shown in Fig. 3. The XRD pattern of a CuS powder reveals seven orientation, (101), (102), (103), (110), (107), (108), and (203) at 2θ equal to 28.0°, 29.26°, 31.18°, 48.20°, 47.54°, 52.04 ° and 58.72 ° which indicate a covellite CuS phase with hexagonal structure, whereas the presence of secondary phase of deginite $Cu_{1.75}S$ was also indicated in the figure, and the planes which corresponds to these diffraction angles are closely corresponding to orthorhombic structure along the (314), (412) at 2θ equals to 49.28°, 50.44°.

The XRD pattern of $Cu_{1.75}S$ phase shows many peaks corresponds to (202), (022), (203), (104), (205), (240), (423) and (430) planes at 2θ equal to 27.44°, 28.36°, 33.70°, 34.74°, 47.14°, 51.92°, 57.93° and 59.09° respectively, confirm that the films belong to the orthorhombic structure. Also there was a secondary phase with peaks for monoclinic phase of Cu_2S along (242) and (080) at 2θ equal to 23.88° and 25.14°, and it had one peak of $Cu_{1.76}S$ along (820) plane at 2θ equal to 26.26°.

The XRD pattern of $Cu_{1.8}S$ phase exhibit five peaks along the (555), (119), (00$\underline{10}$),(220) ,($\underline{11}$ $\underline{11}$ 3) at 2θ equal to 27.18°, 29.12°, 32.24° , 47.58°, 51.94°, these peaks were related to cubic structure of anillite structure. Also one peak presence as a secondary structure for hexagonal phase of CuS along the (203) at 2θ equals to 58.82°.

The XRD pattern of $Cu_{1.95}S$ phase exhibit four peaks for hexagonal $Cu_{1.96}S$ phase along the (031), (220) (141), and (100) at 2θ equal to 20.88°, 22.56°, 31.20°, and 45.12°. The presence of secondary phase of Cu_2S peaks with monoclinic structure can be notes along (232), (024), and (201) at 2θ equal 32.56°, 33.30° and 57.20°, also there were four peaks for hexagonal $Cu_{1.92}S$ phase along (300),(301), (204), and (312) at 2θ equals 26.72°,28.36°, 31.88°, and 35.26°.

Also there are two peaks of $Cu_{1.8}S$ along ($\underline{10}$ $\underline{10}$ 6), and ($\underline{11}$ $\underline{11}$ 3) at 2θ equal to 47.22° and 52.04° and one peak for hexagonal structure of CuS phase along (203) at 2θ equal to 58.32°.

The XRD patterns of Cu_2S phase which has many peaks for Cu_2S phase along (-104), (231), (132), (041), (033), (141), (232), (024), (026), (562) at 2θ equal to 27.0°, 28.6°, 28.92°, 30.92°, 31.58°, 32.04° , 32.54°, 33.04°, 47.46°, and 52.22°, this phase has monoclinic structure with preferred orientation along [026] direction, and one peak for hexagonal CuS phase along (203) at 58.512° , all these result were shown in Table 2. One can see that the obtained powders contains a mixture of copper sulfide phases, this result agrees with the result of Pop et al. [16]. The high copper content phases have problem, which represent by that the copper atoms instability towards the formation of copper vacancies, this leads to the formation of different crystal structures depending on Cu vacancy concentrations [17-19]. A rough estimate of the average crystallite size using the Scherrer formula gives a range of values (4.1-36.9) nm.

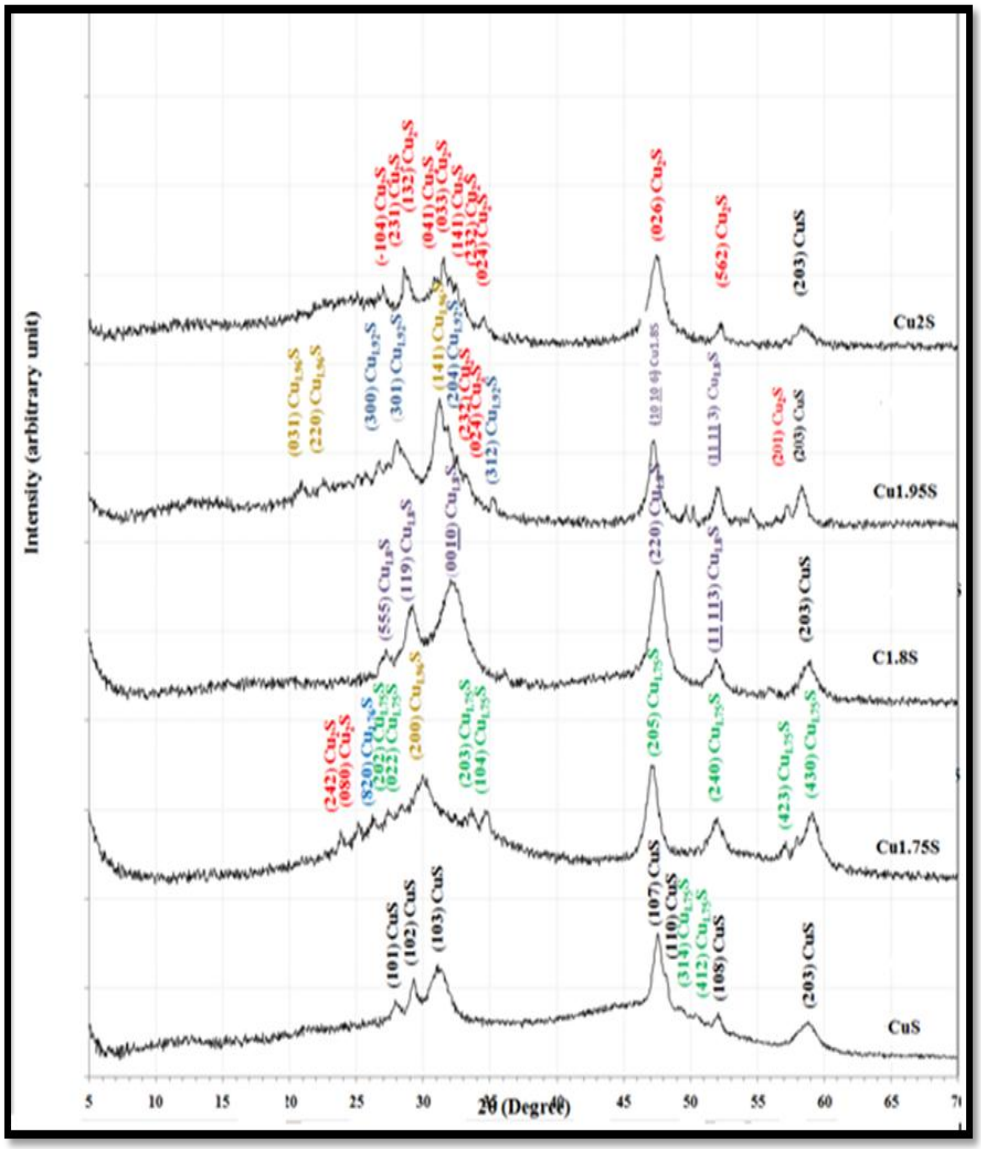

Fig. 3: Crystal structure of $Cu_{2-x}S$ powders at different molar ratio of Cu.

Conclusions

Copper sulfide ($Cu_{2-x}S$) nanoparticles with different molar ratios (Cu/S) were prepared by chemical precipitation. The composition ratio of the elements was slightly deviated from the calculated ratios. Scanning electron microscope images showed uniform surface with agglomerate nanoparticles for all samples. X-ray diffraction analysis of $Cu_{2-x}S$ powders showed that the samples have crystalline structure, and the molar concentration ratio of the precursors was important parameters for synthesizing $Cu_{2-x}S$ powder.

Table 2: Structural of $Cu_{2-x}S$ powders at different molar ratio.

phase	2θ (Deg.)	FWHM (Deg.)	d_{hkl} Exp.(Å)	G.S (nm)	hkl	d_{hkl} Std.(Å)	Phase	Card No.
CuS	28.0000	0.6120	3.1841	13.4	(101)	3.2230	CuS	24-60
	29.2600	0.7682	3.0498	10.7	(102)	3.0480	CuS	24-60
	31.1800	1.6434	2.8662	5.0	(103)	2.8130	CuS	24-60
	47.5400	0.7500	1.9111	11.6	(107)	1.9020	CuS	24-60
	48.2000	0.5880	1.8865	14.8	(110)	1.8960	CuS	24-60
	49.2800	0.5410	1.8476	16.2	(314)	1.8479	$Cu_{1.75}S$	24-58A
	50.4400	0.5410	1.8078	16.2	(412)	1.8069	$Cu_{1.75}S$	24-58A
	52.0400	0.5700	1.7559	15.5	(108)	1.7350	CuS	24-60
	58.7200	1.7242	1.5711	5.3	(203)	1.5720	CuS	24-60
$Cu_{1.75}S$	23.8800	0.3530	3.7233	23.0	(242)	3.7300	Cu_2S	23-961
	25.1400	0.4240	3.5395	19.2	(080)	3.5900	Cu_2S	23-961
	26.2600	0.5650	3.3910	14.4	(820)	3.3500	$Cu_{1.76}S$	23-960
	27.4400	0.5500	3.2478	14.9	(202)	3.2180	$Cu_{1.75}S$	24-58A
	28.3600	0.4240	3.1445	19.3	(022)	3.1900	$Cu_{1.75}S$	24-58A
	30.0300	1.5000	2.9733	5.5	(200)	2.8520	$Cu_{1.96}S$	12-174
	33.7000	0.5600	2.6574	14.8	(203)	2.6870	$Cu_{1.75}S$	24-58A
	34.7400	0.5459	2.5802	15.3	(104)	2.5990	$Cu_{1.75}S$	24-58A
	47.1400	0.9880	1.9264	8.8	(205)	1.9227	$Cu_{1.75}S$	24-58A
	51.9200	1.0908	1.7597	8.1	(240)	1.7553	$Cu_{1.75}S$	24-58A
	57.9312	0.4251	1.5906	21.4	(423)	1.5880	$Cu_{1.75}S$	24-58A
	59.0912	1.2703	1.5621	7.2	(430)	1.5740	$Cu_{1.75}S$	24-58A
$Cu_{1.8}S$	27.1800	0.6807	3.2783	12.0	(555)	3.2100	$Cu_{1.8}S$	23-962
	29.1200	0.9497	3.0641	8.6	(119)	3.0100	$Cu_{1.8}S$	23-962
	32.2400	2.0283	2.7744	4.1	(00$\underline{1}$0)	2.7700	$Cu_{1.8}S$	23-962
	47.5800	1.1737	1.9096	7.4	(220)	1.9690	$Cu_{1.8}S$	23-962
	51.9400	0.9706	1.7591	9.1	($\underline{1}1$ $\underline{1}$13)	1.7520	$Cu_{1.8}S$	23-962
	58.8200	1.3581	1.5687	6.7	(203)	1.5738	CuS	24-60
$Cu_{1.95}S$	20.8800	0.4710	4.2510	17.2	(031)	4.2400	$Cu_{1.96}S$	23-958
	22.5600	0.4470	3.9381	18.1	(220)	3.8800	$Cu_{1.96}S$	23-958
	26.7200	0.5180	3.3336	15.8	(300)	3.2600	$Cu_{1.92}S$	23-958
	28.3600	1.4590	3.1445	5.6	(301)	3.1600	$Cu_{1.92}S$	23-958
	31.2000	0.7760	2.8644	10.6	(141)	2.864	$Cu_{1.96}S$	23-958
	31.8800	0.3400	2.8049	24.3	(204)	2.817	$Cu_{1.92}S$	23-958
	32.5600	0.2242	2.7478	36.9	(232)	2.7318	Cu_2S	33-490
	33.3000	0.5420	2.6884	15.3	(024)	2.6973	Cu_2S	33-490
	35.2600	0.3384	2.5433	24.6	(312)	2.5400	$Cu_{1.92}S$	23-958
	47.2200	0.6761	1.9233	12.8	(10 10 6)	1.9670	$Cu_{1.8}S$	23-958
	52.0400	0.7060	1.7559	12.5	($\underline{1}1$ $\underline{1}1$ 3)	1.7520	$Cu_{1.8}S$	33-490
	57.2000	0.3530	1.6092	25.6	(201)	1.6580	Cu_2S	33-490
	58.3200	0.8700	1.5809	10.5	(203)	1.5730	CuS	33-490
Cu_2S	27.0000	0.3760	3.2997	21.7	(-104)	3.2760	Cu_2S	33-490
	28.6000	0.2820	3.1186	29.1	(231)	3.1210	Cu_2S	33-490
	28.9200	0.2820	3.0849	29.1	(132)	3.0540	Cu_2S	33-490
	30.9200	0.2590	2.8897	31.8	(041)	2.8860	Cu_2S	33-490
	31.5800	0.3060	2.8308	27.0	(033)	2.8267	Cu_2S	33-490
	32.0400	0.3060	2.7912	27.0	(141)	2.7648	Cu_2S	33-490
	32.5400	0.3060	2.7495	27.1	(232)	2.7318	Cu_2S	33-490
	33.0400	0.2820	2.7090	29.4	(024)	2.6973	Cu_2S	33-490
	47.460	1.059	1.9141	8.2	(026)	1.9110	Cu_2S	33-490
	52.220	0.700	1.7503	12.6	(562)	1.7800	Cu_2S	23-961
	58.512	1.300	1.5762	7.0	(203)	1.5738	CuS	24-60

References

[1] A.U Ubale, K.S. Chipade, M.V. Bhute, P.P. Raut, G.P. Malpe, Y.S. Sakhare, M.R. Belkhedkar, International Journal of Materials and Chemistry, 2, 4 (2012) 165-172.

[2] P. A. Ajibade and N. L. Botha, Nanomaterials, 7 (2017) 1-13.

[3] P. Vas-Umnuay and C.-hung Chang, ECS Journal of Solid State Science and Technology, 2 (2013) 120-129.

[4] A. D. Dhondge, S. R. Gosavi, N. M. Gosavi, C. P. Sawant , A. M. Patil, A. R. Shelke, World Journal of Condensed Matter Physics, 5 (2015) 1-9.

[5] S.A. Patil, N. Mengal, A.A. Memon, S.H. Jeong, Journal of Allows and Compounds, 708 (2017) 568-574.

[6] Y. Zhao, H. Pan, Y.Lou, X. Qiu, J. Zhu, and C. Burda, J. AM. Chem. Soc., 131 (2009) 4253-4261.

[7] A. K. Singh, S. Mehra, G.S. Thool European Chemical Bulletin, 2 (2013) 518-523.

[8] A. Astam, Y. Akaltun, M. Yildirim, Turk. J. Phys., 38 (2014) 245-252.

[9] F. A. Sabaha, N. M. Ahmed, Z. Hassan, H. S. Rasheed, Elsevier Procedia Chemistry, 19 (2016) 15-20.

[10] P. Chakraborty, J. Adhikary, S. Chatterjee, B. Biswas, T. Chattopadhyay, RASAYAN J. Chem., 9, 1 (2016) 77-83.

[11] Y. Zhang, Z.-P. Qiao, X.-M. Chen, Journal of Solid State Chemistry, 167, 1(2002) 249-253.

[12] R. Suja, D. Geetha, P. Ramesh, International Journal of Scientific & Engineering Research, 4, 3 (2013) 1-3.

[13] R. Cordova, H. Gomez, R. Schrebler, P. Cury, M. Orellana, P. Grez, D. Leinen, J. R. Barrado, R. Del Río, Langmuir, 18, 22 (2002) 8647-8654.

[14] P. Priyadharshini and R. Revathy, International Journal of Recent Scientific Research, 6, 4 (2015) 3328-3331.

[15] J. Kundu and D. Pradhan, New J. Chem., 37 (2013) 1470-1478.

[16] A.E. Pop, M.N. Batin, V. Popescu, Powder Metallurgy Progress, 11 (2011) 3-4.

[17] A. M. Al-Dhafiri, G. J. Russell, J. Woods, Semiconductor Science and Technology, 7, 8 (1992) 1052-1057.

[18] P. Kumar, R. Nagarajana, R. Sarangi, Journal of Materials Chemistry C, 1, 13 (2013) 2448-2454.

[19] M. Lotfipour, T. Machani, D. P. Rossi, K. E. Plass, Chemistry of Materials, 23, 12 (2011) 3032-3038.